



# Integral field spectroscopy of low- $z$ QSOs and Seyfert galaxies <sup>\*</sup>

## Dependence of EELRs on nuclear properties

Bernd Husemann<sup>1</sup>, Lutz Wisotzki<sup>1</sup>, Sebastian F. Sánchez<sup>2</sup>, and Knud Jahnke<sup>3</sup>

<sup>1</sup> Astrophysikalisches Institut Potsdam, An der Sternwarte 16, 14482 Potsdam, Germany

<sup>2</sup> Centro Astronómico Hispano Alemán de Calar Alto (CSIC-MPIA), E-4004 Almería, Spain

<sup>3</sup> Max-Planck-Institut für Astronomie, Königsstuhl 17, D-69117 Heidelberg, Germany

**Abstract.** We present a preliminary analysis of 20 mainly radio-quiet low- $z$  quasars and 12 Seyfert galaxies observed with an integral field spectrograph. Searching for extended emission-line regions (EELRs) around the active nuclei in these host galaxies, we find a relation between the nuclear properties and the presence of an EELR for both high and low-luminosity AGN. Only those AGN with weak Fe II emission and broad H $\beta$  lines (FWHM > 4000 km/s) show an EELR. Furthermore, we find that the AGN luminosity cannot account for this apparent dichotomy. Differences in the structure of the nuclear region or differences in intrinsic properties of the host galaxies are required to explain our observations.

**Key words.** Galaxies: Active - Quasars: emission-lines - Galaxies: ISM

## 1. Introduction

The interstellar medium (ISM) in the host galaxies of QSOs and Seyfert galaxies can be heated and ionised by the nuclear UV-radiation or by a jet-cloud interaction. So far, mainly radio-loud QSOs (e.g., Crawford & Vanderriest 2000; Stockton et al. 2002; Fu & Stockton 2006) and radio galaxies (e.g. Villar-Martín et al. 2006, 2007) have been studied with integral field spectroscopy

(IFS) to investigate the effect of a jet on its gaseous surrounding. The combined diagnostic power of imaging and spectroscopy allows for a flexible treatment of the data, facilitating the construction of broad- or narrow-band images, or 2-dimensional velocity maps as traced by emission or absorption lines, or the spectral analysis of selected regions within the field of view. We started a programme to systematically study the ionised component of the ISM traced by extended emission-line regions (EELRs) in mainly radio-quiet QSOs and Seyfert galaxies on kpc scales by means of integral field spectroscopy.

---

Send offprint requests to: bhusemann@aip.de

<sup>\*</sup> Based on observations collected at the Centro Astronómico Hispano Alemán (CAHA) at Calar Alto, operated jointly by the Max-Planck-Institut für Astronomie and the Instituto de Astrofísica de Andalucía (CSIC)

## 2. The QSO sample

We targeted a sample of 20 low-redshift ( $z < 0.3$ ) quasars, selected from the Palomar-Green Survey (Schmidt & Green 1983) and from the Hamburg/ESO survey (Wisotzki et al. 2000, Wisotzki et al. in prep.). The QSOs have apparent magnitudes in the range of  $V \sim 14 - 17$ ; corresponding to typical luminosities of  $M_V < -23$ . Three objects are steep-spectrum RLQs, another is classified as a flat-spectrum RLQ; all the other sources are known to be radio-quiet. To our knowledge, this is the largest sample of bright quasars observed with an IFU so far.

We employed the Potsdam Multi-Aperture Spectrophotometer (PMAS; Roth et al. 2005), mounted on the 3.5 m telescope at Calar Alto Observatory. The PMAS lens array was used at a spatial pixel ('spaxel') scale of  $0.5'' \times 0.5''$ , which for  $16 \times 16$  spaxels resulted in a field of view of  $8'' \times 8''$ . At the typical redshifts of our targets we were able to sample the quasar environment with a resolution of  $\sim 1$  kpc, and cover linear extents of up to  $\sim 20$  kpc in diameter. A more detailed description of the results presented here can be found in Husemann et al. (2008).

### 2.1. Narrow-band images

A subsample of  $[\text{O III}] \lambda 5007$  narrow-band images extracted from the IFU datacube are shown in Fig. 1. The nuclear emission was subtracted from the datacubes before using the technique proposed by Christensen et al. (2006). This method gives very good results but a slight over-subtraction is unavoidable at the location of the QSO. We found that 8/20 QSOs show an EELR with linear sizes of the order of 10–20 kpc. Only 3 of them are RLQs and 5 are RQQs. We show here only a subset of 3/12 undetected sources to illustrate the significance of our EELR detections. A few objects overlap with the sample of previous narrow-band imaging studies (Stockton & McKenty 1987; Bennert et al. 2002). We note the HST study by Bennert et al. (2002) resolves mainly high-surface brightness features of the EELRs less than  $1''$  away from the QSO nuclei. The

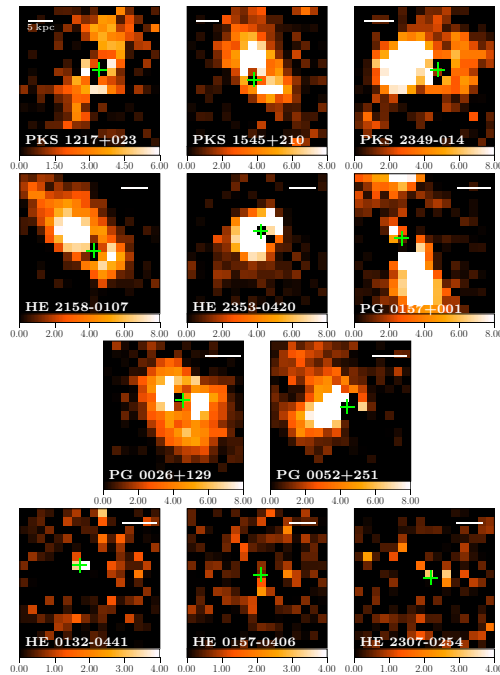


**Fig. 1.** Nucleus-subtracted  $[\text{O III}]$  narrow-band images extracted from the datacubes. All 8 quasars with clearly detected EELR are shown in the top three rows. The bottom row presents three example cases with non-detected EELR for comparison. Note that the apparent holes at most quasar locations are due to oversubtraction and thus not real. The colour coded line flux is in units of  $10^{-16} \text{ erg/s/cm}^2/\text{arcsec}^2$ . The white marker shows a 5kpc linear scale at the quasar redshift.

line ratio  $[\text{O III}]/\text{H}\beta$  is about  $\sim 10$  for all EELRs, implying ionisation by the AGN.

### 2.2. Relation between EELR and QSO properties

In essentially all QSOs where we detected an EELR in  $[\text{O III}]$ , we measured only weak  $\text{Fe II}$  emission in their *nuclear spectra*. Thus, QSOs with and without an EELR populate two distinct groups (Fig. 2) with a cut at  $\log(\text{Fe II EW})=1.4$ . Comparing the EELR  $[\text{O III}]$  flux normalised by the nuclear  $\text{H}\beta$  flux with the FWHM of broad  $\text{H}\beta$  emission line, we found again a clear separation of the two groups at a FWHM of 4000 km/s

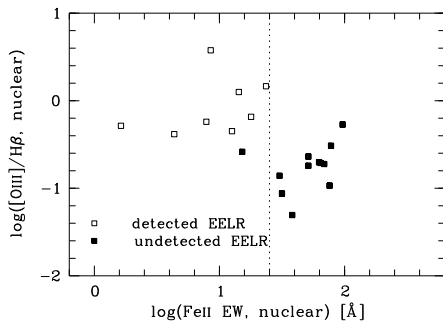


**Fig. 2.** EELR properties are linked with nuclear spectral properties: Nuclear [O III]/H $\beta$  flux ratio vs. the nuclear Fe II EW. The quasars with a detected EELR are denoted by the open squares, the undetected ones are shown as upper limits (filled symbols with arrows down).

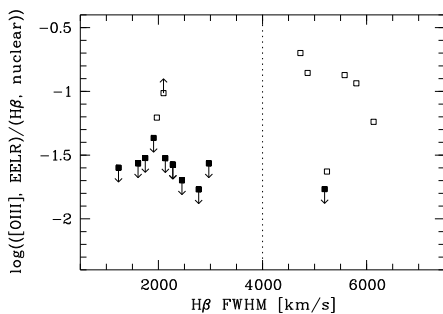


**Fig. 3.** Total EELR flux normalised by the nuclear H $\beta$  flux vs. the FWHM of the broad H $\beta$  component. A dashed line indicates a suggestive separation between the detected and non-detected EELRs. For one object the measured value is shown as lower limit because the EELR is larger than our field of view.

(Fig. 3), albeit with a slightly larger number of interlopers. Boroson & Oke (1984) and Boroson, Persson & Oke (1985) qualitatively found the same dichotomy using off-nuclear long-slit spectroscopy. The apparent advantage of using IFS is that we are now able to recover the overall shape and luminosity of the EELRs.

By exploring more fundamental quantities of the AGN we found that both populations have a similar distribution of continuum luminosities (Fig. 4). Thus, the luminosity of the QSO seems to be not primarily responsible for the presence of an EELR.

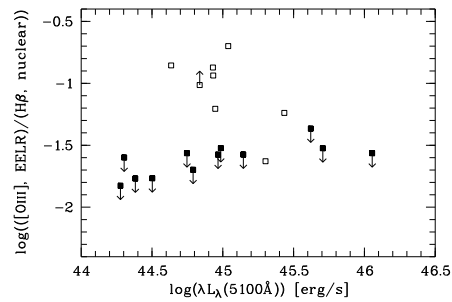


**Fig. 4.** The EELR flux normalised by the nuclear H $\beta$  flux plotted against continuum luminosity at 5100 Å. Symbols, upper and lower limits as in Fig. 3.

### 3. Results from Seyfert galaxies

To extend the range in AGN luminosities, we analysed an X-ray selected sample of nearby Seyfert galaxies observed with the PPAK fibre-bundle of the PMAS IFU. The larger field of view of PPAK (74''  $\times$  65'') and its low spatial resolution (fibre diameter  $\sim$  2.7'') correspond to a similar linear scale and linear resolution at the Seyfert galaxies compared to our QSO observations. Due to the X-ray selection the sample contains not only Seyfert 1 galaxies (8 objects), but also Seyfert 2 galaxies (4 objects). The Seyfert 1 galaxies seem to follow the same relation between EELR and nuclear spectral properties as found for the QSOs. We present preliminary results by comparing the properties of the ISM and the nuclear spectra for the two Seyfert 1 galaxies RBS 1367 (Fig. 5 top panels) and RBS 1545 (Fig. 5 bottom panels). From the line diagnostic diagrams we infer that the ISM near the nucleus of RBS 1367 is ionised predominantly by AGN radiation, while the ISM of RBS 1545 is ionised by star forming region in all parts of the host galaxy. Comparing this with the nuclear spectrum it is clear that only AGN with a broad H $\beta$  line and low Fe II emission can predominantly ionise their surrounding ISM.

### 4. Conclusions

Analysing a sample of low-redshift QSO and local Seyfert galaxies we found that EELRs can be found around high and low luminos-

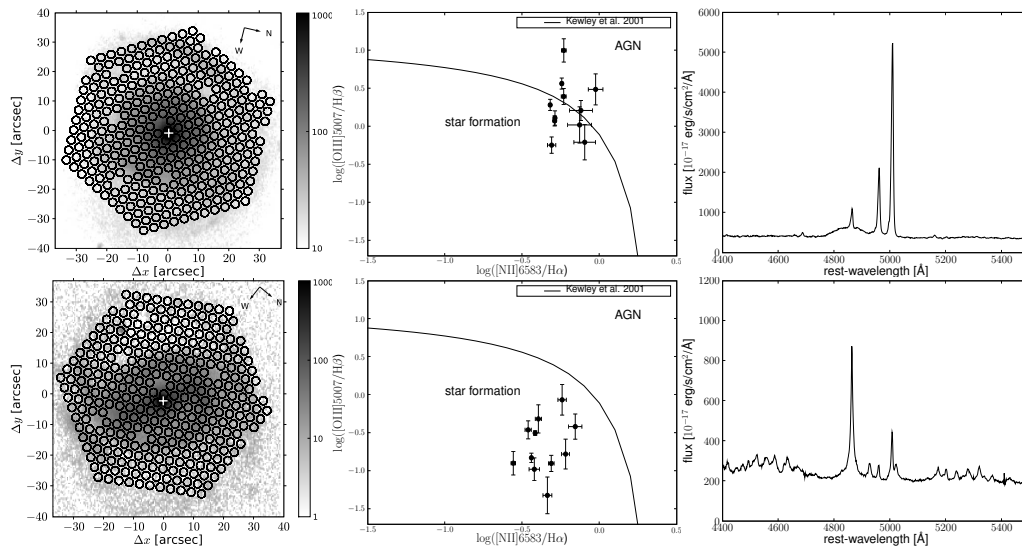


**Fig. 5.** Comparing the ISM and nuclear spectral properties of the Seyfert galaxies RBS 1367 (top) and RBS 1545 (bottom). The left panel show the positions of the fibres over-plotted on an SDSS  $g'$ -band image. Subtracting spectra of single stellar populations from the individual fibre spectra we were able to accurately measure various emission lines to construct a diagnostic diagram (middle panel). The right panel illustrates the different characteristics of the nuclear spectra in the  $H\beta$  region.

ity AGN irrespective of their radio activity. However, the detection of an EELR ionised by the AGN radiation can be linked to the nuclear spectral properties of the AGN itself. It thus appears that we can predict the presence and properties of an EELR already from the nuclear spectrum in QSO and Seyfert galaxies.

This shows that there is a relation between the properties of the sub-pc scale nucleus and the properties of the super-kpc scale ISM in the host galaxy. Since we can basically rule out the AGN luminosity as a driver for this connection, there remain probably only two possibilities: 1. Differences in the structure of the nuclear region (e.g. inclination, torus geometry, jet activity). 2. The properties of the host galaxies of the two classes are intrinsically different. The physical driver for this connection remains unknown and needs further investigation to better understand the role of AGN feedback processes in the evolution of galaxies.

*Acknowledgements.* BH and LW acknowledge financial support by the DFG Priority Program 1177, grant Wi 1369/22-1. KJ acknowledges support through the DFG Emmy Noether-Program.

## References

- Bennert, N. et al. 2002, *ApJ*, 574, L105  
 Boroson, T. A. & Oke, J. B. 1984, *ApJ*, 281, 535  
 Boroson, T. A., Persson, S. E. & Oke, J. B. 1985, *ApJ*, 293, 120  
 Christensen, L., et al. 2006, *A&A*, 459, 717  
 Crawford, C. S. & Vanderriest, C. 2000, *MNRAS*, 315, 433  
 Fu, H. & Stockton, A. 2006, *ApJ*, 650, 80  
 Husemann et al. 2008, *A&A* accepted, [astro-ph:0807.1467](https://arxiv.org/abs/astro-ph/0807.1467)  
 Kewley, L. J. et al. 2001, *ApJ*, 556, 121  
 Stockton, A. & McKenty, J. W. 1987, *ApJ*, 316, 584  
 Stockton, A. et al. 2002, *ApJ*, 572, 735  
 Roth, M. M., et al. 2005, *PASP*, 117, 620  
 Schmidt, M. & Green, R. G. 1983, *ApJ*, 269, 352  
 Villar-Martín, M. et al. 2006, *MNRAS*, 366, L1  
 Villar-Martín, M. et al. 2007, *MNRAS*, 378, 416  
 Wisotzki, L., et al. 2000, *A&A*, 358, 77